An iterative micromechanical modeling to estimate the thermal and mechanical properties of polydisperse composites with platy particles: Application to anisotropic hemp and lime concretes

Sophie Dartois, Sophanarith Mom, Hélène Dumontet, Abdelwahed Ben Hamida

An iterative micromechanical modeling to estimate the thermal and mechanical properties of polydisperse composites with platy particles: application to anisotropic hemp and lime concretes.

Sophie DARTOIS[1], Sophanarith MOM[1], Hélène DUMONTET[1], Abdelwahed BEN HAMIDA[1].

1. Sorbonne Universités, UPMC Univ Paris 06, CNRS, UMR 7190, Institut Jean Le Rond ∂'Alembert, F-75005 Paris, France.

Email addresses: sophie.dartois@upmc.fr (corresponding author), sophanarith.mom@gmail.com, helene.dumontet@upmc.fr, abdelwahed.ben_hamida@upmc.fr.

Abstract

This work aims at providing a multi-scale model to estimate the effective properties of hemp and lime concretes. The microstructures of such materials are characterized by a relatively high filling rate, platy orthotropic particles distributed on a wide range of spatial directions, and a high level of porosity at meso and micro scales. An iterative micromechanical modeling is here enhanced with some numerical features allowing to deal with the shape and orientation of the particles and with the resulting effective anisotropy of concretes. The model thus constructed is first put into practice to identify the properties of hemp shives and air-slaked lime for various compaction degrees. The results obtained are then used as input data to estimate the thermal and mechanical properties of both a collection of moderately compacted concretes, and a set of concretes with several compaction degrees. Simulations results are eventually confronted with experimental data from the literature.

Keywords

Hemp and Lime Concretes, Multiscale Modeling, Anisotropy, Platy Particles, Porosity, Finite Element Analysis, Microstructure, Homogenization, Polydisperse Composites.

1. Introduction

Over the past thirty years building materials reinforced with vegetal products, and more specifically vegetal concretes, have made a remarkable headway in the construction field due to their slight environmental impact. Hemp and lime concretes, also known as hempcretes, are one of the most commonly used bio-based construction material for walls since their outbreak in the late 1980s [46], [21]. Not only are they made of sustainable resources usually considered as by-products of the fiber and oil industries, but their production has a very low carbon footprint. They have also proved to be particularly efficient as far as thermal insulation is concerned allowing thus some substantial energy savings [10], [22], [21], [12]. On the other hand, their mechanical performances stay rather modest which explains why they are currently only used as filling materials for walls, roofs and floors, together with wooden load-bearing structures. Vegetable concrete manufacturers in association with project managers aim at improving the mechanical resistance of vegetable concretes while preserving the insulation properties of the latter. They also need the establishment of building norms that will enable a wide use of this new type of materials. Comprehensive constitutive models can provide valuable help to make this step easier. They allow indeed to perform collections of numerical simulations (so called "digital experiments") with varying parameters, such as the physical nature, shape or spatial arrangement of the constituents. In the framework of a large optimization and certification campaign, the purpose of this work is to predict the thermal and mechanical properties of hemp and lime concretes at the end of their manufacturing process by means of a numerical multi-scale modeling technique. Such technique allows to pay a special attention to the quite complex microstructures of this class of materials.

Hemp-lime concretes (HLC) are obtained by mixing hemp hurds commonly referred to as hemp shives with a lime based binder. The latter is an air-slaked lime produced in presence of pozzolans, and water. The mixture obtained is then processed and casted (which often includes a compaction stage) and is eventually dried. The very nature of the material and its manufacturing process make several modeling issues arise.
First of all the specific morphology and spatial distribution of hemp shives have to be taken into account. Hemp shives are indeed elongated platy particles cut in the wooden core of the plant stem. They have a rectangular parallelepipedic shape with a moderate slenderness Fig.1(b). Hemp shives exhibit an orthotropic behavior as they are bored through by micro tubular ducts originally forming the sap distribution network. The spatial arrangement of shives together with their own behavior is at the origin of the material global anisotropy. The compaction phase of the manufacturing process tends moreover to align shives in several parallel planes or strata, in-

creasing thus a potential initial anisotropy [29], [39], [44]. The architecture of the material also depends on the concrete formulation, i.e. on the quantities of shives and lime introduced. Some hemp and lime concretes may appear as an entanglement of hemp particles maintained together thanks to local lime bridges when the shives rate is high, whereas others have a more classical microstructure, i.e. hemp particles embedded in a lime matrix phase Fig.1(a).
A related issue to deal with is the high porosity rate as it may represent up to 70% of the concretes volume [5], [18], and sometimes nearly 80% [19], [13]. Pores and voids are indeed present at both meso and microscales. Mesopores (i.e. whose size is close to the size of hemp shives) can be the result of the very architecture of the material when the lime rate is low. They appear as well in the matrix phase when the lime rate is high and the forming process lacks mixing. As noted earlier tubular microvoids can also be observed in shives. The porosity of hemp shives is indeed commonly considered as a little higher than 80% [25], [33]. Some micropores may as well appear in the lime matrix as the result of chemical reactions during the drying phase. The presence of these two categories of voids (mesopores and micropores) and their potential closure during the compaction phase of the manufacturing process has to be taken into account in the constitutive modeling of the hemp concretes in use [15].
Scale transition modeling techniques including morphology features appear thus as an appropriate tool to account for all these complex morphological effects when trying to estimate the properties of hempcretes.

Micromechanical models have been developed over the past sixty years to determine the global behavior of heterogeneous materials depending on their local microstructures. A series of models can be found in the literature using analytical homogenization schemes, often based on the fundamental Eshelby's ellipsoidal inclusion model [17]. Very few are nevertheless dedicated to materials reinforced with rectangular parallelepipedic particles more or less randomly distributed in the material, for which analytical solutions are missing [6], [23], [24]. As computational resources increase numerical full-field finite element simulations on detailed Representative Volume Elements (RVE) could appear as a convenient solution to this problem. The RVE could either be numerically designed or digitally reconstructed from experimental imagery like computed tomography. In both cases, the generation of the RVE reveals itself quite complex when dealing with contacts between the particles and the size of the RVE as evidenced by several articles on fibrous media and especially wood-based ones [26], [43], [27], [40], [16] among others. As a consequence the filling rates of the materials numerically designed from scratch are generally below those of the category of concretes considered here. In the case of computed tomography, computer resources needed are high for both the reconstruction phase and the subsequent finite

(a) Close up of a hemp and lime concrete sample

(b) Hemp shives covered with lime

Figure 1: Hemp concrete sample and corresponding particles (hemp shives).

element solving procedure. But the most limitating fact in the use of this type of approach is that the meshing step entails some remodeling of the real microstructure in order to avoid distorted elements and mesh size problems. Some microstructural artefacts are therefore artificially added to RVE potentially with an effect on the identification of the global properties of the material.
As the materials at stake in this paper do not have a precisely controlled microstructure given their forming process it is here chosen, as several authors did previously [4], [12], [2], to focus on much more time efficient modeling methods.

More precisely this paper deals with an iterative multiscale modeling which has been developed to describe the behavior of highly-filled materials with polydispersed heterogeneities. The approach at stake is inspired by the differential scheme defined by McLaughlin [28], enhanced by Norris [31] and proposed for linear porous media by Zimmerman [47]. The modeling pro-

cedure follows the manufacturing process of granular composites materials in which heterogeneities are gradually introduced in a matrix phase whose properties evolve through the process. The creation of a given medium is thus achieved through the sequential production of intermediate partially-filled media. The effective constitutive laws (as defined by [34], [20], [1]), of the corresponding intermediate composite can be obtained thanks to any homogenization technique since the volume fraction of heterogeneities is very small for a given step. This method was first proposed for non linear and porous media such as clayes [11] and dealt with composites with identical particles. It was next extended to non-linear media such as porous media [8], [37] or periodic damaged cemented soils [9]. In the meantime the approach was extended to study polydisperse composites such as syntactic foams [48]. It is nevertheless to be noted that the papers listed above dealt either with materials with spherical inclusions, allowing thus an analytical solution of the local problem, or with periodic materials.

The modeling purpose of the present work is therefore to widen the scope of the iterative multiscale modeling to materials with platy particles of various geometrical dimensions, orientations and physical properties with a special attention paid to the resulting anisotropy of the effective macroscopic behavior of the composites. To this aim the model is coupled with dedicated finite element simulations and analytical procedures allowing to take into account the orientation of the particles in the material. The main features of these procedures are presented in Section 2. Simulations are then carried out in Section 3 with the aim of estimating the thermal and mechanical linear effective properties of hemp and lime concretes. The results stemming from these simulations are eventually confronted to experimental data from the literature. More precisely the iterative multiscale modeling is first put into practice to identify the properties of the constituents of hempcretes for various compaction degrees. The results obtained are then used as input data to estimate the thermal and mechanical properties of a collection of moderately compacted concretes on the one hand, and of a specific concrete being subjected to increasing compaction degrees during its manufacturing phase on the other hand.

2. Model description and implementation

2.1. General framework of the iterative multiscale modeling

The iterative multiscale modeling follows the manufacturing process of granular composites materials and is schematically represented on Fig.2. As stated in the previous section it is inspired by the differential scheme [28]. At each step j a composite material is created by adding a small fraction $\delta f^{(j)}$ of inclusions (pores or particles) in a consistent matrix phase. A structural analysis, commonly referred to as "local problem", is then performed on the

corresponding Representative Volume Element (RVE) in order to determine its effective thermal and mechanical behavior.

Thanks to a homogenization procedure the properties of an equivalent homogeneous medium are identified and the latter is finally used as the matrix phase for the following step. This process is repeated n times until the targeted filling rate $f = \sum_{j=1}^{n} \delta f^{(j)}$ is reached, and the filling rate at step j is:

$$f^{(j)} = \frac{\delta f^{(j)}}{(1-f) + \sum_{p=1}^{j} \delta f^{(p)}} \tag{1}$$

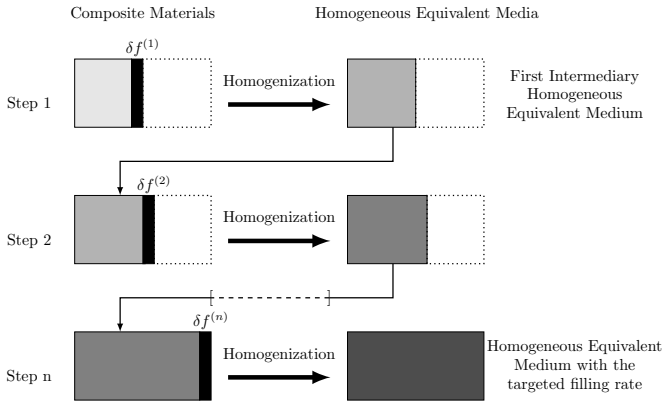

Figure 2: Basic principle of the iterative homogenization technique.

In a thermal linear framework, at each step j of the iterative procedure, the Representative Volume Element (RVE) noted Ω is submitted to a macroscopic thermal gradient $\underline{G}$. This induces a microscopic heat flux $\underline{q}(\underline{x})$ which depends on the position $\underline{x} \in \Omega$ and whose variations in each phase are described thanks to the Fourier law of heat conduction:

$$\underline{q}(\underline{x}) = -\boldsymbol{K}^{\alpha}(\underline{x})\, \underline{grad}\, T(\underline{x}), \quad \underline{x}\ in\ \Omega^{\alpha}, \quad \alpha \in \{m, inc\} \tag{2}$$

with α equal to m standing for matrix, or to inc for inclusion. Ω^{α} is the volume of the phase α in the RVE $\left(\Omega = \Omega^{m} \cup \Omega^{inc}\right)$. $T(\underline{x})$ is the temperature at point $\underline{x}$ in Ω, and $\boldsymbol{K}^{\alpha}$ is the second order tensor of thermal conductivity in phase α.

The equivalent second order conductivity tensor $\boldsymbol{K}^{*(j)}$ to determine at each homogenization step j links the macroscopic temperature gradient $\underline{G}$

to the macroscopic flux $\underline{Q}^{(j)}$ thanks to Eq (3):

$$\underline{Q}^{(j)} \;=\; \left\langle\, \underline{q}^{(j)}(\underline{x}) \right\rangle \;=\; -\boldsymbol{K}^{*(j)}.\left\langle\, \underline{grad}\, T^{(j)}(\underline{x}) \,\right\rangle \;=\; -\boldsymbol{K}^{*(j)}.\underline{G} \qquad (3)$$

where $\langle . \rangle$ denotes classical volume average.

$\boldsymbol{K}^{*\,(j)}$ explicitly depends on the properties of the phases of the local problem, i.e. $\boldsymbol{K}^{\alpha}, \alpha \in \{m, inc\}$. The iterative principle implies that for a given step j, the conductivity tensor of the matrix phase $\boldsymbol{K}^{m}$ corresponds to the homogenized conductivity tensor identified at the end of the previous step $\boldsymbol{K}^{*(j-1)}$, namely $\boldsymbol{K}^{m} = \boldsymbol{K}^{*(j-1)}$. As a consequence, the equivalent behavior searched at step j has the following form inspired by the classical solution by Eshelby [17]:

$$\boldsymbol{K}^{*\,(j)} = \boldsymbol{K}^{*\,(j-1)} + f^{(j)}\left(\boldsymbol{K}^{inc} - \boldsymbol{K}^{*\,(j-1)}\right) : \left\langle\, \boldsymbol{a}^{(j)}\left(\underline{x}, f^{(j)}, \boldsymbol{K}^{inc}, \boldsymbol{K}^{*(j-1)}\right) \right\rangle_{\Omega^i} \qquad (4)$$

where $\boldsymbol{K}^{inc}$ is the conductivity tensor of the inclusion added (with $\boldsymbol{K}^{inc} = \boldsymbol{K}^{air}$ if the inclusion added at step j is a pore), and $\boldsymbol{a}^{(j)}$ represents the localization tensor at step j.

In a linear elastic context the same representative volume element Ω is considered. A distinction is nevertheless here made between pores with no rigidity Ω^p, elastic inclusions Ω^{inc}, and the matrix Ω^m $\left(\Omega = \Omega^p \cup \Omega^{inc} \cup \Omega^m\right)$. The RVE is submitted to a macroscopic strain $\mathbf{E}$ which causes microscopic stress and strain fields, respectively $\boldsymbol{\sigma}(\underline{x})$ and $\boldsymbol{\varepsilon}(\underline{x})$, to appear in the RVE. They are locally linked via the rigidity tensor of each phase: $\mathbb{C}^{\alpha}(\underline{x})$, with once again α equal to m for matrix, or inc for inclusion.

$$\boldsymbol{\sigma}(\underline{x}) = \mathbb{C}^{\alpha}(\underline{x}) \,:\, \boldsymbol{\varepsilon}(\underline{u}), \qquad \underline{x} \in \Omega^{\alpha},\ \alpha \in \{m, inc\} \qquad (5)$$

The equivalent fourth order rigidity tensor $\mathbb{C}^{*(j)}$ to determine at the end of each homogenization step j links the macroscopic stress tensor $\boldsymbol{\Sigma}^{(j)}$, which is the classical volume average of the microscropic stress field $\boldsymbol{\sigma}^{(j)}(\underline{x})$, to the macroscopic strain field applied on the RVE thanks to the relationship Eq (6):

$$\boldsymbol{\Sigma}^{(j)} = \left\langle \boldsymbol{\sigma}^{(j)}(\underline{x}) \right\rangle \;=\; \mathbb{C}^{*(j)} \,:\, \mathbf{E} \;=\; \mathbb{C}^{*(j)} \,:\, \left\langle\!\left\langle\, \boldsymbol{\varepsilon}(\underline{u}^{(j)}) \,\right\rangle\!\right\rangle \qquad (6)$$

where $\langle\langle\, \boldsymbol{\varepsilon}(\underline{u}) \,\rangle\rangle$ is the average of local strains $\boldsymbol{\varepsilon}(\underline{x})$ in a RVE containing pores.
In a similar way as the thermal context, the homogenized tensor $\mathbb{C}^{*(j)}$ explicitly depends on the rigidity tensor at step $j-1$ since $\mathbb{C}^{m} = \mathbb{C}^{*(j-1)}$.
If the inclusion added to the matrix at step j is an elastic particle with a rigidity tensor $\mathbb{C}^{inc}$, the equivalent behavior at this step has the following

form:

$$\mathbb{C}^{*(j)} = \mathbb{C}^{*(j-1)} + \varphi^{(j)} \left(\mathbb{C}^{inc} - \mathbb{C}^{*(j-1)} \right) : \left\langle \, \mathbb{A}^{(j)} \left(\underline{x}, f^{(j)}, \mathbb{C}^{inc}, \mathbb{C}^{*(j-1)} \right) \right\rangle_{\Omega^{inc}} \tag{7}$$

where $\varphi^{(j)}$ is the volume fraction of elastic particles in the composite at step j and $\mathbb{A}^{(j)}$ represents the strain localization tensor. Note that if $\phi^{(j)}$ is the volume fraction of pores in the composites at step j then $f^{(j)} = \varphi^{(j)} + \phi^{(j)}$. If a pore is added to the matrix phase at step j, the equivalent behavior is given by:

$$\mathbb{C}^{*(j)} = \mathbb{C}^{*(j-1)} - \phi^{(j)} \mathbb{C}^{*(j-1)} : \left\langle \left\langle \, \mathbb{A}^{(j)} \left(\underline{x}, f^{(j)}, \mathbb{C}^{*(j-1)} \right) \right\rangle \right\rangle_{\Omega^p} \tag{8}$$

In this iterative homogenization procedure, the volume fraction of heterogeneities in each local problem to solve is very small. As a consequence the properties of the successive homogeneous media defined in Eqs (3) or (6) can be identified regardless of the homogenization technique used to this aim. More precisely, all the classical Eshelby based homogenization methods, even the original dilute scheme [17], can be put into practice at each step with similar results on the effective properties of the final composite as evidenced in the literature [8]. It is yet to be noted that the filling rate at the end of the whole procedure can reach any level, including the highest ones (i.e. superior to 80%).

The iterative structure of the multiscale modeling considered makes it moreover particularly convenient and efficient when it comes to estimate the behavior of highly-filled materials with multiphysic and complex microstructures. The fraction of heterogeneity introduced at each step can indeed vary in shape, size, nature and orientation from one step to another. An illustration of this major asset can be found in [48] where the iterative multiscale modeling was used to estimate the behavior of syntactic foams which are highly contrasted and polydispersed composites. Another example is the work on cemented soils (pores and sand) [41], in which the nature of the inclusion varied from one homogenization step to another. The results thus obtained were in good concordance with experimental results in both studies; but it is to be noted that the investigations were limited to isotropic materials with spherical inclusions. In order to estimate the thermal and mechanical characteristics of materials with elongated platy shaped particles such as hemp-lime concrete or any other morphological features, finite element simulations and other extra subroutines are developed and coupled to the iterative scheme. They are detailed in the following section starting with the description of the real geometry of the particles.

2.2. Coupling with Finite Element Analysis to account for the shape of particles

The iterative multiscale scheme described in subsection 2.1 does not depend on the solving procedure used for the local structure problem at each step j. For materials with spherical or ellipsoidal inclusions analytical models are particularly efficient, but when heterogeneities are polyhedral, the use of numerical solving methods is necessary. This is the case of materials filled with rectangular parallelepipedic particles on which this study is focused. A first step to improve the iterative multiscale method is consequently to combine it with Finite Element Analysis (FEA) simulations when solving each intermediate local problem. In practice, at each step j a local problem is solved on a RVE by doing the following:

1. The RVE is composed of a single oriented parallelepipedic particle, embedded in a matrix phase.

2. Since the modeling scheme does not depend in its principle on the geometry nor on the slenderness of the particle, and since the estimation of the properties of hemp concretes is eventually at stake in this study the shape factor of the particle introduced at each step is close to the one of hemp shives Fig.3(a). For more precisions on hemp shives granulometry one can refer to [7], [44], [19], [14], [35].

3. The spatial orientation of the particle is characterized by the three angles θ, ψ and φ defined on Fig.3(b).

4. The properties of the matrix phase are updated at each step (i.e. chosen equal to the homogenized behavior obtained at step $j-1$).

5. The global size of the RVE is accommodated in order that the volume fraction of particles in the material is $f^{(j)}$ at the end of the step.

At the end of the process one obtains the equivalent homogeneous orthotropic behavior of a media filled with a targeted proportion f of particles all oriented in the same direction. This media will be referred to as a *single-oriented* material throughout the paper.

In order to avoid the creation of a collection of meshes each corresponding to a possible orientation of the particle, a reference mesh, partially represented on Fig.3(c), is used together with rotation matrices $\mathbf{P}(\theta, \psi, \varphi)$. Those matrices allow indeed to deduce the effective properties of a material containing a particle in an arbitrary direction (θ, ψ, φ) from those of a material with a single particle whose axes are aligned with the ones of the RVE i.e. $(\theta = 90°, \psi = 0°, \varphi = 0°)$.
In the thermal framework, the effective conductivity tensor of a material

with a particle in an arbitrary direction can thus be obtained by using the following relationship: $\mathbf{K}^*(\theta, \psi, \varphi) = \mathbf{P}^T\, \mathbf{K}^*(90°, 0°, 0°)\, \mathbf{P}$.

The same process can be used in an elastic context to obtain the effective rigidity tensor $\mathbb{C}^*(\theta, \psi, \varphi) = \mathbf{P}^T\, (\mathbf{P}^T\, \mathbb{C}^*(90°, 0°, 0°)\, \mathbf{P})\, \mathbf{P}$.

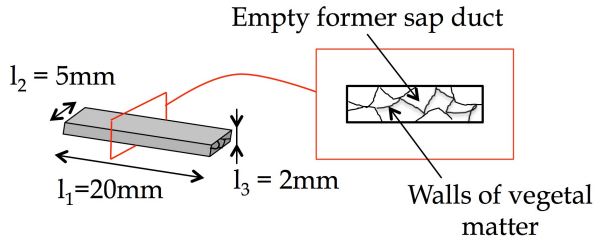

(a) Definition of the particles structure and geometric parameters

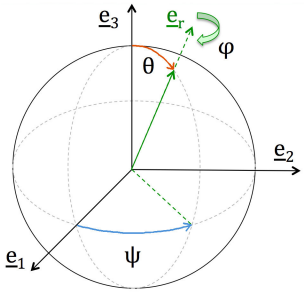

(b) Definition of orientation angles

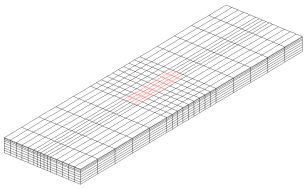

(c) Slice of the reference mesh used, with a particle oriented in the direction ($\theta = 90°, \psi = 0°, \varphi = 0°$)

Figure 3: Definition of the RVE and the geometry of the particles used for the resolution of the local problem at each step j.

The implementation of this digital process was validated thanks numerical simulations run on a virtual orthotropic test material in which all the particles have the exact same geometry and are aligned in the same direction $\theta = 90°, \psi = 0°, \varphi = 0°$. The results of these simulations were compared with salient results from simulations run on periodic microstructures in both thermal an elastic frameworks. For low filling rates both methods provide the same results in terms of effective conductivities and elastic properties. For higher filling rates the periodic approach is yet limited because of mesh distorsion when particles get too close.

2.3. Orientation of the particles and potential induced anisotropy

The case of more complex microstructures is logically debated in this subsection. More precisely, the composites considered here are made of a

matrix phase containing a large number of particles oriented in m distinct directions. They will be referred to as *poly-oriented* materials as opposed to *single-oriented* materials defined in Section 2.2. Families of particles are also defined, each family corresponding to one of the m orientations classically defined by the three angles (θ, ψ, φ) represented on Fig.3(b).

A scenario for the introduction of the particles is here proposed. It is inspired in its principle by the methodology used when dealing with the granulometric polydispersion of hollow spheres in syntactic foams [48]. In the present study the orientation of the particles is the discriminating parameter rather than the size of the particles, leading to some adjustments. From this point, for an easier description of how the iterative method can be used to model poly-oriented materials it is chosen to present its practical application on materials containing particles evenly distributed on the m spatial directions, meaning that all the families contain the same number of particles. It is yet to be noted that this is absolutely not a restriction of the model. In the specific case of particles evenly distributed on m directions the iterative modeling is composed of n series of m successive homogenization substeps each one performed with a particle belonging to a different family as illustrated on Fig.4. If f is the overall volume fraction of particles in the composite, then the proportion of family i is $f_i = f/m$, and the volume fraction of particles introduced during an homogenization substep is therefore $\delta f_i = f_i/n = f/(n \times m)$. At the end of each series of homogenization the symmetries of the final intermediate equivalent homogeneous material depend on the number and orientation of the families as well as on the intrinsic behavior of the particles.

In the special case of fully isotropic materials the number of families m tends to infinity and the effective behavior of the final intermediate equivalent homogeneous material at the end of a series k is expected to be isotropic. As a consequence it can be obtained thanks to a single simulation on a RVE with a particle oriented in the direction $(90°, 0°, 0°)$ followed by, first the use of the rotation matrix as described in Section 2.2, and then an integration phase on the three angles covering all the spatial directions instead of a succession of m homogenization steps. In the thermal context for instance the effective conductivity $\mathbf{K}^*$ of the intermediate homogeneous medium at the end of a series k can thus be obtained in practice thanks to the following explicit integral :

$$\begin{aligned} \mathbf{K}^* &= \frac{1}{2\pi^2} \int_0^{2\pi} \left(\int_0^{2\pi} \left(\int_0^{\pi} \sin\theta \; \mathbf{P}^T(\theta,\psi,\varphi) \; \mathbf{K}^*(90°,0°,0°) \; \mathbf{P}(\theta,\psi,\varphi) \; d\theta \right) d\varphi \right) d\psi \\ &= \frac{1}{3} \left(K^*_{11}(90°,0°,0°) + K^*_{22}(90°,0°,0°) + K^*_{33}(90°,0°,0°) \right) \boldsymbol{Id} \end{aligned} \tag{9}$$

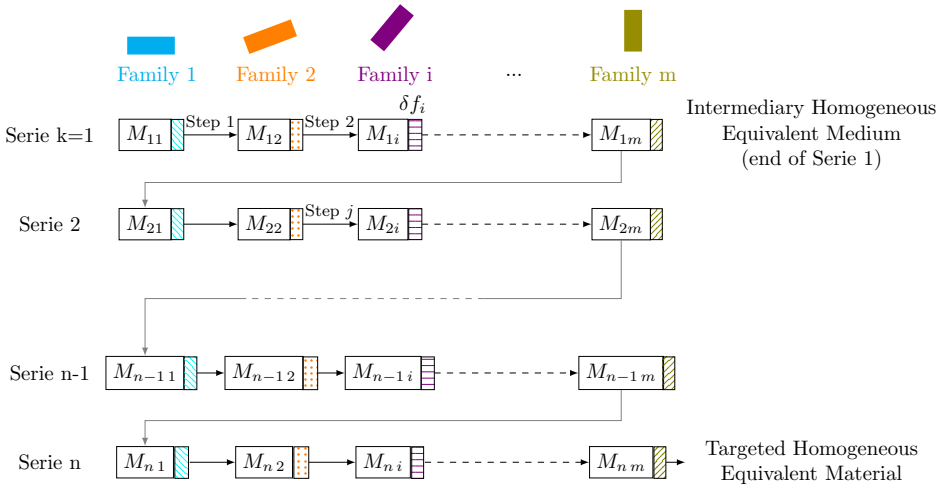

Figure 4: Schematic representation of the iterative addition of particles depending on their families in the digital multiscale modeling. M_{11} = pristine matrix phase, M_{ki} = intermediary homogeneous equivalent medium at step $j = k \times i$.

where $\boldsymbol{Id}$ stands for the identity matrix.

In the linear elastic context, the isotropic rigidity tensor $\mathbb{C}^*$ at the end of a series k and its representative matrix $\mathbf{C}^*$ are classically expressed as functions of Lamé coefficients λ and μ which are themselves obtained thanks to the components of the intermediate effective rigidity tensor $\mathbb{C}^{*90} = \mathbb{C}^*(90°, 0°, 0°)$ as follows :

$$\lambda = \frac{1}{15}\left(C_{11}^{*90} + C_{22}^{*90} + C_{33}^{*90}\right) + \frac{4}{15}\left(C_{12}^{*90} + C_{13}^{*90} + C_{23}^{*90}\right) - \frac{2}{15}\left(C_{44}^{*90} + C_{55}^{*90} + C_{66}^{*90}\right)$$

$$2\mu = \frac{1}{15}\left(C_{11}^{*90} + C_{22}^{*90} + C_{33}^{*90} - C_{12}^{*90} - C_{13}^{*90} - C_{23}^{*90}\right) + \frac{1}{5}\left(C_{44}^{*90} + C_{55}^{*90} + C_{66}^{*90}\right)$$

It is worth mentioning that another scenario could have been envisioned for the introduction of the particles by inverting the nesting order of the loops on the families and on the increments of the iterative modeling itself. This alternate scenario has been tested on fully isotropic materials during Mom's Ph.D. and the results obtained have been compared to those given by classical analytical solutions for materials filled with spherical inclusions. For a contrast higher to ten between particles and matrix in terms of thermal conductivity and Young modulus the alternate scenario leads to incorrect results in terms of effective properties, with a relative error superior to 10% when compared to results obtained thanks to the scenario represented on Fig.4 and the analytical solving.

On Fig.5 are reported the results obtained for a contrast on Young modulus close to 350 (mechanical properties listed in Table 1). The mechanical properties of a particle of hemp wood (hemp shiv) have been identified from the properties of loose shives thanks to an inverse method in which loose shives are considered as a two phased material (hemp particles + air) whose effective properties are known. The iterative micromechanical modeling was used to identify which values of Young modulus and Poisson coefficient for hemp particles lead to the experimentally identified macroscopic isotropic properties of loose shives. The results obtained were similar to those calculated by Cerezo in her Ph.D. work thanks to a self-consistent scheme.
Fig.5 shows, as expected, that in the case of isotropic media the volume fraction of particles has an impact on the effective global behavior but not the shape nor dimension of the particles. The relative error between results from numerical simulations run on materials with elongated particle randomly distributed and analytical solutions remains indeed inferior to 2% for the whole range of filling rate.

Phase	**Young Modulus (MPa)**	**Poisson ratio**
Matrix	500	0.2
Particle	1.5	0.1

Table 1: Mechanical properties of the phases used for digital validation of the iterative micromechanical modeling.

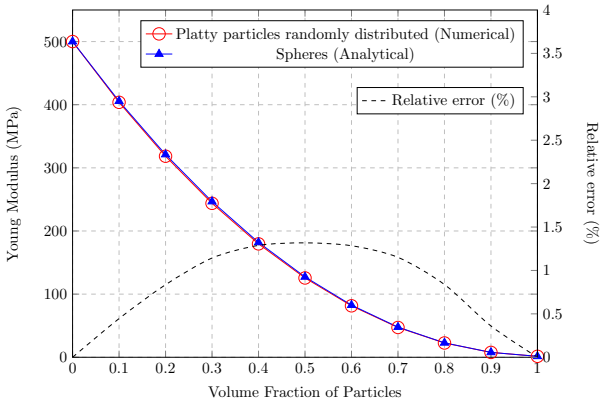

Figure 5: Comparison of the global Young modulus of an isotropic random material obtained thanks to the numerical iterative modeling (elongated platty particles randomly distributed) and thanks to analytical solving (spheres).

A sensitivity study has also been carried out regarding the size of the increment δf_i representing the volume fraction of heterogeneities included

in the matrix phase at each step. This study showed that for an increment $\delta f_i = 1\%$ the relative error between the results stemming from both scenari is less than 3% within the range of contrast between the phases usually encountered in hemp and lime concretes. $\delta f = 1\%$ is therefore the value chosen for all the simulations presented in this paper.

For composites with a limited number of material symmetries, a combination of the methods described in the previous paragraphs can be used. For instance an estimation of the global behavior of a transverse isotropic composite can be obtained thanks to Eq.(9) with $\theta = 90°$ and without integrating over θ when the isotropy is in plane $(\underline{e}_1, \underline{e}_2)$. The behavior within the isotropy plane corresponds then to the one of a composite reinforced by circular inclusions, but the estimation of the behavior off axis requires a 3D numerical solving.

When materials are purely anisotropic due to a discrete spatial orientation of particles, a homogenization step is carried out on a RVE containing a single particle, then the effective thermal and mechanical behaviors of intermediate media each corresponding to a family of particles are obtained thanks to rotation matrices. Then the effective global linear behavior of the composite is eventually estimated via a weighted summation on the various intermediate $\mathbf{K}^*$ and $\mathbb{C}^*$ whose weights correspond to the volume fraction of the particles in each direction.

2.4. Influence of the nature and behavior of the phases on effective properties.

The discreet process on which the iterative multiscale modeling is based proves itself very convenient when it comes to study composites containing inclusions of different natures such as pores and elastic particles. The mechanical or thermal properties of the inclusion can indeed be modified at each homogenization step just like its orientation was in the previous section. The question of the introduction sequence of the various inclusions is then raised. One can either choose to alternate the introduction of the inclusions or to introduce all the particles of a given type in a row. In a linear framework and for the category of materials eventually at stake, i.e. hemp concretes, simulations results indicate that the introduction sequence has a very limited impact on the effective anisotropic properties (and especially when the contrast is reduced as it is the case in the thermal case). This is why this point is not investigated here. In Sections 3.2 and 3.3 an alternate introduction of phases (hemp shives and pores) is carried out for all simulations. Issues concerning the orientation and nature of particles are consequently addressed the same way.

The numerical solving of the local problems developed in Section 2.2 allows as well to take into account the presence of interphases between particles and matrix in an explicit manner. Accounting for the interphase only requires to create an actual layer of elements around the particle in the digital RVE on which each local problem is solved. The introduction of interphases within the iterative multiscale modeling has been briefly investigated in the form of a feasibility study. Simulations have been successfully performed on virtual study materials constituted of an isotropic matrix filled with particles wrapped in an interphase with a few number of elements through its constant thickness; the latter being set to ensure that the volume of the interphase is equal to the volume of the particle. This configuration has been chosen on the basis of micrographies of plant-based concretes [32], [15]. In vegetal concretes the porosity of particles makes it indeed possible for some water sorption to happen during the manufacturing phase of the concretes. This water may later be evacuated leading to the formation of a halo of modified matrix around the particles. The presence of this interphase tends to lower the global mechanical properties of concretes and should be accounted for when trying to estimate the global rigidity of hemp concretes, but one of the current impediment to the continuation of the numerical modeling work undertaken on the subject is the lack of experimental identification for the mechanical and thermal properties of the interphases. Meanwhile solutions are sought after in order to prevent this phenomenon from happening, for instance by waterproofing particles before mixing thanks to wax coats [3], or by chemical treatments [38].
The numerical multiscale modeling developed here makes it possible as well to take into account the intrinsic anisotropic behavior of the particles. In order to validate this point simulations have been carried out to estimate the effective behavior of a single-oriented composite (i.e. composed of a matrix phase containing platy particles and all oriented in the same direction). In a first test case particles are isotropic whereas in a second test case particles are transverse isotropic, with the orthotropy axes matching the geometrical symmetry axes of the particles. The corresponding thermal properties are listed in Table 2.

Phase	**Conductivity** $(W.m^{-1}.K^{-1})$
Isotropic Matrix	0.240
Isotropic Particles	0.102
Transverse Isotropic Particles	0.112 (longitudinal) 0.095 (transverse)

Table 2: Thermal properties of the phases used for digital validation of the iterative micromechanical modeling

Results obtained are shown on Fig.2.4. As expected, the anisotropy is increased when the particles are transverse isotropic. When the filling rate

is equal to one, the effective behavior of the oriented composite obviously matches the behavior of the particles. This is of course due to the fact that the orthotropy axes match the loading axes in that case. These results prove if needed the necessity to consider the anisotropy of particles as a major input data when modeling oriented materials, and show the ability of the digital procedure to account for it.

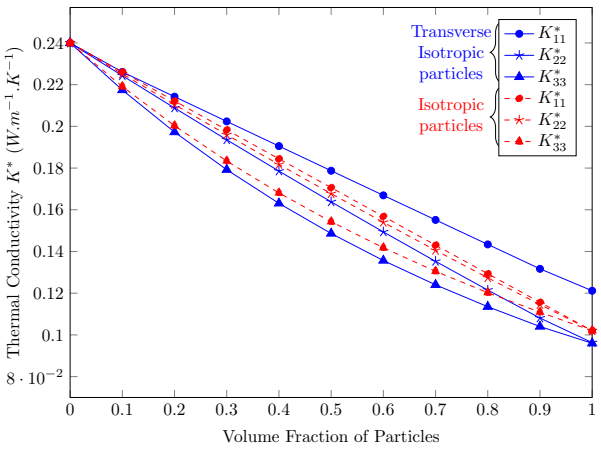

Figure 6: Comparison of the effective properties of two single-oriented composites filled with isotropic or transversally isotropic platy particles. Results obtained by digital simulation with the iterative modeling.

3. Estimate of thermal and elastic properties of hemp concretes.

A wide range of hemp concretes mixes exist depending on their final use (floors, walls, roofs, coating,...). They mainly differ in terms of filling and compaction rates (i.e. density and manufacturing process). Simulations, have been performed in both thermal and elastic contexts, in order to estimate the effective properties of a collection of hemp concretes thanks to the iterative multiscale model whatever the compaction rates of the different concretes are. Composites studied here are on the one hand concretes in which the spatial distribution and orientation of the particles is even in each direction and on the other hand concretes with a high compaction rate such as breeze blocks or laboratory samples.

3.1. Preliminary identification of the behavior of the constituents

One of the most popular lime matrix used for the manufacture of hemp concretes is Tradical ®PF70 whose thermal conductivity and mechanical properties are close to those reported in Table 1 & 2. Lime matrix is here

considered as a microporous material. In order to take into account the evolution of the properties of the lime matrix with respect to its porosity rate, simulations have been carried out with the numerical iterative multiscale model on RVEs composed of a spherical pore embedded in a lime matrix phase. The isotropic thermal and mechanical properties obtained for air-slaked lime are displayed on Fig.7(a) and Fig.7(b) (right ordinate axis).

The identification of the behavior of shives is more complicated since it is quite difficult to perform experiments on a single hemp shiv given its size. Several authors have chosen to identify the properties of the wooden particles from data collected on loose shives samples by using an inverse analysis. A first estimate can indeed be obtained by considering loose shives as a heterogeneous two-phase material made of shives embedded in an air matrix and by using various homogenization schemes. The thermal and mechanical properties of a hemp particle can for instance be determined thanks to a self-consistent scheme based on a RVE with spherical inclusions randomly distributed in space as it was done in Cerezo's Ph.D. work partially reported in [4]. The iterative numerical multiscale modeling can also be used under the same assumptions and with the same input data. This leads to similar results as the ones obtained by Cerezo (reported in Tables 1 and 2) when considering the particle isotropic: $E_{\text{part.}} = 1.5MPa$ and $\nu_{\text{part.}} = 0.1$, $k_{\text{part.}} = 0.110\, W.m^{-1}.K^{-1}$.
This identification can nevertheless be enhanced by taking into account the heterogeneity and anisotropy of hemp shives. Hemp shives can schematically be seen as a bundle of connected micro-ducts made of vegetal matter and filled with air [29], [13], [36]. The properties of the vegetable matter constituting the walls of the ducts can be estimated by performing an inverse analysis on a two-phase isotropic medium (air and vegetal matter). The volume fractions of both phases in a non compacted state are identified of thanks to measures on density found in the literature [29] (volume fractions: $f_{\text{air}} \simeq 78\%$ and $f_{\text{vege. matter}} \simeq 22\%$). As ducts are parallel, the longitudinal behavior of the hemp particle (ducts direction) is obtained via a classical weighted average on the behavior of the constituents (example for thermal conductivity: $k^{\text{longi.}}_{\text{particle}} = f_{\text{vege. matter}} \cdot k_{\text{vege. matter}} + f_{\text{air}} \cdot k_{\text{air}}$). The 2D version of the iterative multiscale modeling is eventually used to determine the transverse behavior. With this method, the complete effective transverse isotropic behavior of a hemp particle is obtained ranging from its free state to a highly compacted state (i.e. no porosities), as shown on Fig.7(a) and Fig.7(b) (left ordinate axis) together with results obtained for the lime matrix.

The evolution of the thermal and elastic properties of hemp shives and lime with respect to porosity is clearly non-linear. As expected the spindle shaped curves depicting the behavior of transverse isotropic hemp shives

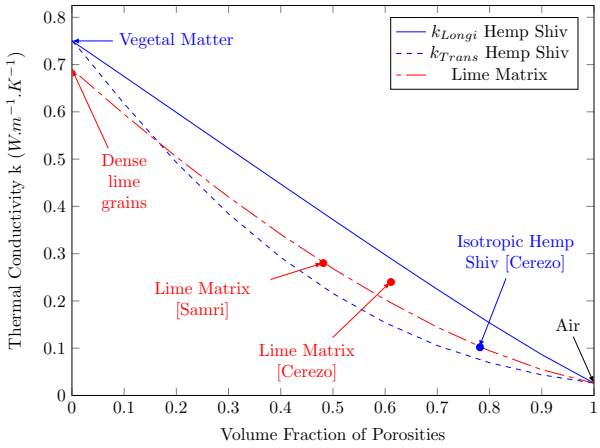

(a) Thermal conductivity

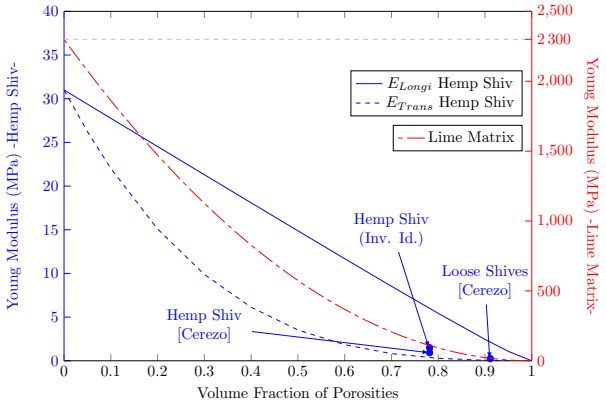

(b) Young Modulus

Figure 7: Transverse isotropic behavior of a hemp particle (shiv) with respect to porosity rate identified thanks to the iterative multiscale modeling (experimental results from Cerezo's Ph.D. work and Samri's master's thesis.).

frame the results found in the literature when considering the particles isotropic. The latter where obtained via an inverse identification from experimental results on loose shives using a self-consistent scheme on a material with spherical particles. As far as the isotropic lime matrix is concerned the results obtained almost interpolate the isolated results obtained by the same authors.

3.2. Thermal conductivity of moderately to highly compacted hemp concretes

The numerical iterative multiscale modeling is here put into practice to estimate the thermal behavior of moderately to highly compacted concretes. This type of concrete is supposed to be transversely isotropic because of

the anisotropic behavior of hemp particles combined with their spatial rearrangement in strata during the compaction phase of their elaboration as exhibited by [29], [45]. The global thermal conductivities obtained are all compared to experimental data collected by Nguyen during his Ph.D. and which are partially reported in [29].

As a first step the numerical iterative multiscale modeling is used to estimate the thermal conductivities of a set of compacted concretes which differ by their formulations (i.e. by the number and volume fractions of their phases), and by their levels of total porosity. It is to be noted that in the literature, concretes formulations are given for a pre-mix state, whereas the simulations presented here require the exact composition after the drying phase. As a consequence the formulation of each concrete of this first set has been identified thanks to inverse methods starting from a measure of the final density of the concrete studied, coupled with an assumption on the distribution of pores in the material. Low density hemp concretes (namely with a density inferior to $500\,kg.m^{-3}$) are here supposed to be three-phased materials constituted of porous lime matrix, porous shives and mesoscopic pores which are approximately the same size as hemp particles; whereas concretes with a higher density (namely with a density superior to $500\,kg.m^{-3}$) are a here considered as a mix of lime and shives only, each with a decreasing porosity with respect to the compaction rate. The decline of intrinsic microporosity in the matrix phase and shives when density increases must be taken into account [42]. It is here achieved thanks to an update of their thermal and mechanical properties following the curves presented on Fig.7(a).
The estimates obtained with the numerical iterative multiscale modeling are reported on Fig.8. The thermal conductivities at the end of the elaboration phase are estimated in the longitudinal direction of the concretes (i.e. compaction direction) as well as the transverse direction of the concretes (i.e. isotropy or strata planes). The results obtained demonstrate first the ability of the iterative multiscale modeling to account for the geometry of the particles and the anisotropy induced by their morphology and spatial arrangement, an element which had not been tested in the previous non numerical versions of the model. From a quantitative point of view, the values obtained frame the results analytically obtained by Cerezo thanks to a self consistent scheme applied to a material with spherical particles (values added on the graph). For a density close to $400\,kg.m^{-3}$ the results numerically obtained surround as well the values experimentally obtained on slightly tamped samples regarded as isotropic materials [14]. These values ranged indeed from 0.105 to $0.116\,W.m^{-1}.K^{-1}$. In addition the results obtained by simulation follow the overall trend of the experimental data obtained on anisotropic samples [29], especially for the lowest densities which correspond in general to the lowest compaction rates. The discrepancies observed here for the formulations with a higher density are therefore attributed to a lack

of information concerning the real initial composition of the corresponding concretes after the drying phase. The formulations identified may indeed slightly differ from the exact composition of the experimental samples.

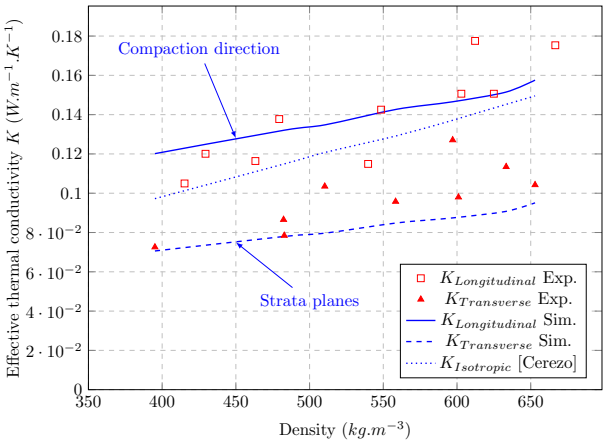

Figure 8: Global thermal behavior of hemp concretes with a moderate compaction rate with respect to their density. Comparison between experimental results [29] and results obtained with the numerical iterative multiscale modeling as well as an analytical solving with a self-consistent scheme from Cerezo's Ph.D. work.

As a second step the numerical iterative multiscale modeling has been used to estimate the global thermal properties of a given set of hemp concretes not only after their elaboration but also throughout a compaction phase. An example of the results obtained is reported on Fig.9. Three levels of compaction are simulated for a given initial formulation. The levels of compaction correspond to the compaction levels for which the properties of the corresponding concretes were experimentally measured [29]. For each measure, the porosity level has once again been updated with the assumption of a progressive closure of mesoscopic pores followed by a progressive closure of the intrinsic microporosities of the phases [42]. The evolution of the microscopic porosity in the constituents is also accounted for by an update of their properties throughout the simulations, following the non linear curves presented on Fig.7(a).
The agreement with the experimental data is here very satisfactory for both longitudinal and transverse directions. One would also notice that, as expected, the compaction phase whose aim is to increase mechanical properties tends to reduce the insulation efficiency of hemp concretes. The numerical iterative multiscale model could therefore be used on a digital benchmark to help identifying the best compromise between thermal and mechanical properties.

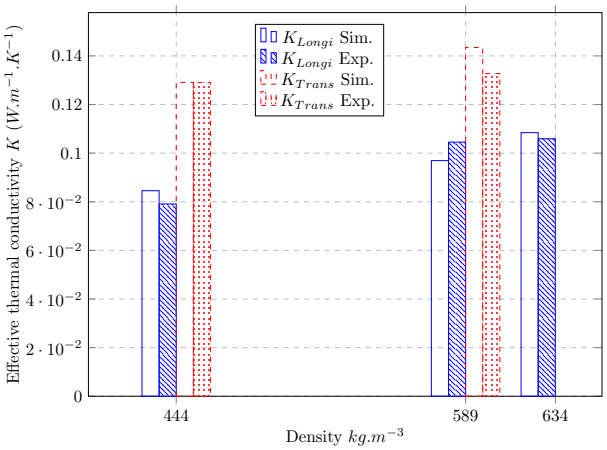

Figure 9: Global thermal behavior of a specific hemp concrete with respect to their density (proportional to compaction rate). Comparison between experimental results [29] and results obtained with the numerical iterative multiscale modeling.

3.3. Elastic rigidity of moderately to highly compacted hemp concretes

In this section, are presented simulations whose aim is to estimate the macroscopic mechanical properties of moderately to highly compacted hemp concretes. Simulations based on the numerical iterative multiscale model are once again performed on a set of concretes which are supposed to have a transverse isotropic global behavior due to the alignment of shives in strata. The formulation of the set of concretes at stake has been priorly estimated thanks to an inverse analysis and thanks to a scenario of pores closure during the compaction phase as it has been done for the estimation of the thermal global properties. The anisotropic behavior of hemp shives described in Section 3.1 is taken into account. Finally, when dealing with the highest compaction rates envisioned (i.e. concretes with the highest densities), the appropriate mechanical properties for the constituents are selected using the results reported on Fig.7(b).

The results obtained for two specific formulations defined in [29] are reported on Fig.10 and are compared to the results experimentally obtained by the corresponding authors. For the lowest densities (i.e. for the lowest compaction rates), the Young modulus obtained for the longitudinal direction (i.e. compaction direction) and the transverse directions (isotropy or strata planes) surround the value statistically obtained from a large collection of samples extracted from batches prepared in numerous independent laboratories [30]. In this study the Young Modulus of hemp concrete treated as an isotropic material ranges from 30 MPa to 40 MPa for a density close to $500\,kg.m^{-3}$. For the highest densities the results presented on Fig.10 show a good concordance between numerical estimates (solid lines) and experimental measures (dotted lines) [29], and this for both types of formulations

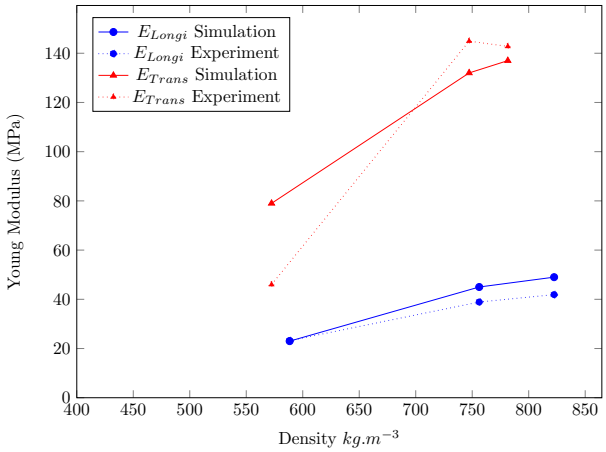

(a) Formulation BAA-BBA-BCA according to Nguyen's classification

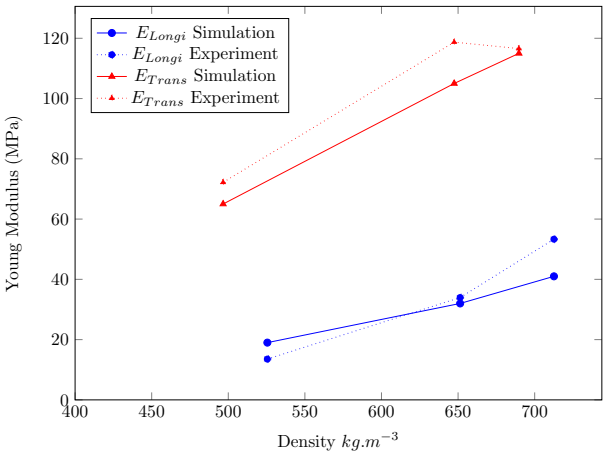

(b) Formulation BAC-BBC-BCC according to Nguyen's classification

Figure 10: Transverse isotropic behavior of two formulations of hemp concretes with respect to their density identified thanks to the numerical iterative multiscale modeling. Comparison with experimental results by Nguyen [29]

considered here. These results show thus the ability of the numerical iterative multiscale modeling to account for the global anisotropy of compacted concretes. They also show the necessity to take into account the anisotropic behavior of shives and most of all pore closures in the estimate the behavior for concretes with a high compaction rate.

4. Conclusion

In this paper was presented an iterative multiscale modeling including finite element simulations on uncluttered meshes allowing to take into account the shapes an orientations of rectangular parallelepipedic particles as well as their influence on the effective global anisotropy of the composites studied. The iterative multiscale modeling has then been put into practice to estimate, in a tridimensional context, the thermal conductivity and elastic rigidity of hemp and lime concretes subjected to a compaction phase during their elaboration. The study of such category of concretes required a preliminary complete inverse identification of the behavior of their constituents in a compacted context since microporosities in shives and lime matrix collapse during the compaction process. This stage was performed thanks to the extended numerical iterative multiscale modeling itself. Simulations were then run to estimate the conductivity and rigidity of moderately and highly compacted concretes microstructures; both of them being transversely isotropic because of a distribution in strata of hemp shives during the compaction phase, and because of the anisotropic behavior of hemp particles. First, the iterative process proved itself efficient to estimate the effective conductivity of a group of concretes with various unrelated formulations and a moderate compaction rate. Then it was used to estimate the effective conductivity and effective rigidity of a smaller set of concretes but for increasing compaction rates. In both cases the results obtained successfully matched experimental data found in the literature. A better precision could nevertheless be obtained thanks to a better identification of the formulations of the composites after the compaction phase and a better experimental identification of the behavior of the phases.
Now that the numerical iterative multiscale modeling has been implemented, tested and validated, it needs to be extended in order to simulate the complete non linear behavior of the composites. The non linearity can be of various origins such as thermo and hygromechanics effects, outbreak of microcracks in the matrix phase or the evolution of the microstructure. The evolution of the size and number of porosities, in the course of a loading case has nevertheless already been accounted for in this study via the evolution of the properties of the constituents. The iterative multiscale modeling has formerly been used to describe materials experiencing diffuse isotropic damage as in the work by Vu *et al.* [41]. The coupling between non linear homogenization methods such as secant method and the iterative method in its numerical version is currently investigated paying ample attention to anisotropy. The results will be communicated in a future paper.

[1] J. Aboudi, *Mechanics of composite materials: a unified micromechanical approach.* Amsterdam: Elsevier Science Publishers, 1991.

[2] A. Akkaoui, S. Caré, and M. Vandamme, "Experimental and micromechanical analysis of the elastic properties of wood-aggregate concrete," *Construction and Building Materials*, vol. 134, 2017. [Online]. Available: http://dx.doi.org/10.1016/j.conbuildmat.2016.12.084

[3] A. Al-Mohamadawi, K. Benhabib, R. Dheilly, and A. Goullieux, "Influence of lignocellulosic aggregate coating with paraffin wax on flax shive and cement-shive composite properties," *Construction and Building Materials*, vol. 102, pp. 94–104, 2016. [Online]. Available: http://dx.doi.org/10.1016/j.conbuildmat.2015.10.190

[4] L. Arnaud and V. Cérézo, "Mechanical, thermal, and acoustical properties of concrete containing vegetable particles," in *Innovations in design with emphasis on seismic, wind, and environmental loading: quality control and innovations in materials/hot-weather concreting*, ser. American concrete Institute special publication, vol. 209, 2002, pp. 151–168.

[5] L. Arnaud and E. Gourlay, "Experimental study of parameters influencing mechanical properties of hemp concretes," *Construction and Building Materials*, vol. 28, pp. 50–56, 2012. [Online]. Available: http://dx.doi.org/10.1016/j.conbuildmat.2011.07.052

[6] L. Banks-Sills, V. Leiderman, and D. Fang, "On the effect of particle shape and orientation on elastic properties of metal matrix composites," *Composites Part B*, vol. 28, no. 4, pp. 465–481, 1997.

[7] S. Benfratello, C. Capitano, G. Peri, G. Rizzo, G. Scaccianoce, and G. Sorrentino, "Thermal and structural properties of a hemp-lime biocomposite," *Construction and Building Materials*, vol. 48, pp. 745–754, 2013. [Online]. Available: http://dx.doi.org/10.1016/j.conbuildmat.2013.07.096

[8] A. Benhamida, I. Djéran-Maigre, H. Dumontet, and S. Smaoui, "Clay compaction modelling by homogenization theory," *International Journal of Rock Mechanics and Mining Sciences*, vol. 42, pp. 996–1005, 2005. [Online]. Available: http://www.doi.org/10.1016/j.ijrmms.2005.05.021

[9] F. Bouchelaghem, A. Benhamida, and H. Q. Vu, "Nonlinear mechanical behaviour of cemented soils," *Computational Materials Science*, vol. 48, no. 2, pp. 287–295, April 2010. [Online]. Available: https://doi.org/10.1016/j.commatsci.2010.01.009

[10] M. Boutin, C. Flamin, S. Quinton, and G. Gosse, "Etudes des caractéristiques environnementales du chanvre," Ministère de l'agriculture et

de la pêche - DPEI - INRA de Lille, Technical Report MAP 04 B1 05 01, September 2006.

[11] A. Brini, F. Pradel, A. Benhamida, and H. Dumontet, "Aging damage of immersed syntactic foams under coupled effects of pressure and aqueous corrosion," in *Fourteenth International Conference on Composite Materials*, San Diego, USA, July 2003.

[12] F. Collet and S. Pretot, "Thermal conductivity of hemp concretes: variation with formulation, density and water content," *Construction and Building Materials*, vol. 65, pp. 612–619, 2014. [Online]. Available: http://dx.doi.org/10.1016/j.conbuildmat.2014.05.039

[13] F. Collet, J. Chamoin, S. Pretot, and C. Lanos, "Comparison of the hygric behaviour of three hemp concretes," *Energy and Buildings*, vol. 62, pp. 294–303, 2013. [Online]. Available: http://dx.doi.org/10.1016/j.enbuild.2013.03.010

[14] P. de Bruijn and P. Johansson, "Moisture fixation and thermal properties of lime-hemp concrete," *Construction and Building Materials*, vol. 47, pp. 1235–1242, 2013. [Online]. Available: http://dx.doi.org/10.1016/j.conbuildmat.2013.06.006

[15] Y. Diquelou, E. Gourlay, L. Arnaud, and B. Kurek, "Influence of binder characteristics on the setting and hardening of hemp lightweight concrete," *Construction and Building Materials*, vol. 112, pp. 506–517, 2016. [Online]. Available: http://dx.doi.org/10.1016/j.conbuildmat.2016.02.138

[16] J. Dirrenberger, S. Forest, and D. Jeulin, "Towards gigantic rve sizes for 3d stochastic fibrous networks," *International Journal of Solids and Structures*, vol. 51, pp. 359–376, 2014. [Online]. Available: http://dx.doi.org/10.1016/j.ijsolstr.2013.10.011

[17] J. D. Eshelby, "The determination of the elastic field of an ellipsoïdal inclusion and related problems," *Proceedings of the Royal Society of London*, vol. 241, no. 1226, 1957. [Online]. Available: http://dx.doi.org/10.1098/rspa.1957.0133

[18] A. Evrard, "Transient hygrothermal behaviour of hemp-lime materials," Ph.D. dissertation, Ecole polytechnique de Louvain Unité d'architecture., 2008.

[19] P. Glé, E. Gourdon, and L. Arnaud, "Acoustical properties of materials made of vegetable particles with several scales of porosity," *Applied Acoustics*, vol. 72, pp. 249–259, 2011. [Online]. Available: http://dx.doi.org/10.1016/j.apacoust.2010.11.003

[20] Z. Hashin, "The elastic moduli of heterogeneous materials," Division of Engineering and Applied Physics, Harvard University, Tech. Rep., September 1960.

[21] C. Ingrao, A. Lo Giudice, J. Bacenetti, C. Tricase, G. Dotelli, M. Fiala, V. Siracusa, and C. Mbohwa, "Energy and environmental assessment of industrial hemp for building applications: A review," *Renewable and Sustainable Energy Reviews*, vol. 51, pp. 29–42, November 2015. [Online]. Available: http://dx.doi.org/10.1016/j.rser.2015.06.002

[22] K. Ip and A. Miller, "Life cycle greenhouse gas emissions of hemp-lime wall constructions in the uk," *Resources, Conservation and Recycling*, vol. 69, pp. 1–9, September 2012. [Online]. Available: http://dx.doi.org/10.1016/j.resconrec.2012.09.001

[23] E. Lacoste, S. Fréour, and F. Jacquemin, "On the validity of the self-consistent scale transition model for inclusions with various morphologies." *Mechanics of Materials*, vol. 42, no. 218-226, 2010. [Online]. Available: https://doi.org/10.1016/j.mechmat.2009.10.002

[24] E. Lacoste, S. Fréour, and F. Jacquemin, "A multi-scale analysis of materials reinforced by inclusions randomly oriented in the ply plane," *Applied Mechanics and Materials*, vol. 61, pp. 55–64, 2011.

[25] C. Lanos, F. Collet, G. Lenain, and Y. Hustache, *Formulation and Implementation (in Bio-aggregate-based Building Materials).* Wiley-ISTE, 2013, ch. 4.

[26] J. Lux, C. Delisée, and X. Thibault, "3d characterisation of wood based fibrous materials: an application," *Image Anal. Stereol.*, vol. 25, pp. 25–35, 2006. [Online]. Available: https://doi.org/10.5566/ias.v25.p25-35

[27] F. Malmberg, J. Lindbald, C. Östlund, K. Almberg, and E. Gamstedt, "Measurement of fibre-fibre contact in three-dimensional images of fibrous materials obtained from x-ray synchrotron microtomography," *Nuclear Instruments and Methods in Physics Research A*, vol. 637, pp. 143–148, January 2011. [Online]. Available: https://doi.org/10.1016/j.nima.2011.01.080

[28] R. McLaughlin, "A study of the differential scheme for composite materials," *International Journal of Engineering Sciences*, vol. 15, no. 237-244, 1977. [Online]. Available: https://doi.org/10.1016/0020-7225(77)90058-1

[29] T. T. Nguyen, V. Picandet, P. Carre, T. Lecompte, S. Amziane, and C. Baley, "Effect of compaction on mechanical and thermal properties of hemp concrete," *European Journal of environmental and*

civil engineering, vol. 14, no. 5, pp. 545–560, 2010. [Online]. Available: http://dx.doi.org/10.1080/19648189.2010.9693246

[30] C. Niyigena, S. Amziane, A. Chateauneuf, L. Arnaud, L. Bessette, F. Collet, C. Lanos, G. Escadeillas, M. Lawrence, C. Magniont, S. Marceau, S. Pavia, U. Peter, V. Picandet, M. Sonebi, and P. Walker, "Variability of the mechanical properties of hemp concrete," *Materials Today Communications*, vol. 7, pp. 122–133, 2016. [Online]. Available: http://dx.doi.org/10.1016/j.mtcomm.2016.03.003

[31] A. N. Norris, "A differential scheme for the effective moduli of composites," *Mechanics of Materials*, vol. 4, pp. 1–16, 1985.

[32] V. Nozahic, S. Amziane, G. Torrent, K. Saïdi, and H. de Baynast, "Design of green concrete made of plant derived aggregates and pumice-lime binder," *Cement and concrete composites*, vol. 34, pp. 231–241, 2012. [Online]. Available: https://doi-org.insis.bib.cnrs.fr/10.1016/j.cemconcomp.2011.09.002

[33] V. Picandet, *Characterization of Plant-Based Aggregates (in Bio-aggregate-based Building Materials)*. Wiley-ISTE, 2013, ch. 2.

[34] A. Rocha and A. Acrivos, "On the effective conductivity of dilute dispersions: general theory for inclusions of arbitrary shape," *Quarterly Journal of Mechanics and Applied Mathematics*, vol. 26(2), 1973. [Online]. Available: http://dx.doi.org/10.1093/qjmam/26.2.217

[35] I. Schwarzova, J. Cigasova, and N. Stevulova, "Thermal stress effect on density changes of hemp hurds composites," *SSP - Journal of Civil Engineering*, vol. 11, no. 2, pp. DOI: 10.1515/sspjce–2016–00 019, 2016.

[36] I. Schwarzowá, "Investigation of observed changes in treated hemp hurds," *GeoScience Engineering*, vol. 62, no. 3, pp. DOI : https://doi.org/10.1515/gse–2016–0021, 2017.

[37] S. Smaoui, A. Benhamida, I. Djeran-Maigre, and H. Dumontet, "Micro-macro approaches coupled to an iterative process for nonlinear porous media," *Computers, Materials & Continua*, vol. 4, no. 3, pp. 153–162, 2006. [Online]. Available: http://www.techscience.com/doi/10.3970/cmc.2006.004.153.pdf

[38] N. Stevulova, J. Cigasova, P. Purcz, I. Schwarzova, F. Kacik, and A. Geffert, "Water absorption behavior of hemp hurds composites," *Materials*, vol. 8, no. 5, pp. 2243–2257, doi:10.3390/ma8052243 2015.

[39] P. Tronet, T. Lecompte, V. Picandet, and C. Baley, "Study of lime hemp concrete (lhc) - mix design, casting process and mechanical behaviour."

Cement and Concrete Composites, vol. 67, pp. 60–72, 2016. [Online]. Available: http://dx.doi.org/10.1016/j.cemconcomp.2015.12.004

[40] J. Viguié, P. Latil, L. Orgéas, P. Dumont, S. Rolland du Roscoat, J. Bloch, C. Marulier, and O. Guiraud, "Finding fibres and their contacts within 3d images of disordered fibrous media," *Composites Science and Technology*, vol. 89, pp. 202–210, 2013. [Online]. Available: http://dx.doi.org/10.1016/j.compscitech.2013.09.023

[41] Q. H. Vu, F. Bouchelaghem, and A. Ben Hamida, "A micromechanical numerical modelling approach for the homogenization of grouted sands." *International Journal Computer Applications in Technology*, vol. 34, no. 1, pp. 72–82, 2009.

[42] R. Walker, S. Pavia, and R. Mitchell, "Mechanical properties and durability of hemp-lime concretes," *Construction and Building Materials*, vol. 61, pp. 340–348, 2014. [Online]. Available: http://dx.doi.org/10.1016/j.conbuildmat.2014.02.065

[43] T. Walther, K. Terzic, T. Donath, H. Meine, F. Beckmann, and H. Thoemen, "Microstructural analysis of lignocellulosic fiber networks," in *Developments in X-Rays Tomography V*, U. Bonde, Ed., vol. 6318. SPIE, 2006.

[44] J. Williams, M. Lawrence, and P. Walker, "A method for the assessment of the internal structure of bio-aggregate concretes." *Construction and Building Materials*, vol. 116, pp. 45–51, May 2016. [Online]. Available: http://dx.doi.org/10.1016/j.conbuildmat.2016.04.088

[45] ——, "The influence of the casting process on the internal structure and physical properties of hemp-lime." *Materials and Structures*, vol. 50:108, December 2017.

[46] T. Woolley, *Low Impact Building*. John Wiley & Sons, 2013.

[47] R. Zimmerman, "Elastic moduli of a solid containing spherical inclusions," *Mechanics of Materials*, vol. 12, no. 17-24, 1991. [Online]. Available: https://doi.org/10.1016/0167-6636(91)90049-6

[48] R. Zouari, A. Ben Hamida, and H. Dumontet, "A micromechanical iterative approach for the behaviour of polydispersed composites," *International Journal of Solids and Structures*, vol. 45, no. 11-12, pp. 3139–3152, 2008. [Online]. Available: https://doi.org/10.1016/j.ijsolstr.2008.01.016